


Ising model for the freezing transitionJacobico Troncoso^{*} and Claudio A. Cerdeiriña[†]*Instituto de Física e Ciencias Aeroespaciais da Universidade de Vigo and Unidad MSMN Asociada al CSIC por el IQF Blas Cabrera, Ourense 32004, Spain* (Received 30 March 2023; revised 10 July 2023; accepted 10 December 2023; published 18 January 2024)

We introduce a three-state Ising model with entropy-volume coupling suitably incorporating a packing mechanism into a lattice gas with no attractive interactions. On working in a great grand canonical ensemble in which the energy, volume, and number of particles are all allowed to fluctuate simultaneously, the model's mean-field solutions illuminate a strictly first-order transition akin to hard-sphere freezing while describing the thermodynamics of solid and fluid phases. Further implementation of attractive interactions in a natural way allows every aspect of the phase diagram of a simple substance to be reproduced, thereby accomplishing the van der Waals picture of the states of matter from first principles of statistical mechanics. This fairly accurate qualitative description plausibly renders mean-field theory a reasonable approach for freezing in three dimensions. At the same time, our mean-field treatment itself suggests freezing to persist in infinitely many dimensions, as advanced from recent simulations [Charbonneau *et al.*, *Eur. Phys. J. E* **44**, 101 (2021)].

DOI: [10.1103/PhysRevE.109.014123](https://doi.org/10.1103/PhysRevE.109.014123)**I. INTRODUCTION**

An outstanding question to the theory of condensed matter is the statistical-mechanical characterization of the solid-liquid transition that ordinary substances are known to undergo. The status of the problem by the mid-1970s is summarized in Ashcroft and Mermin [1] by a seven-line statement indicating that only “very crude” theories exist. Shortly afterward, the theory of topological order showed that melting in $d = 2$ dimensions is triggered by an equilibrium concentration of dislocation defects [2], while computation of phase diagrams from classical density functional theory became notorious [3]. Nevertheless, despite progress, no definite theory for $d = 3$ (and higher dimensions) currently exists.

Our incomplete understanding even concerns the most elementary hard-sphere system: while its freezing transition was revealed long ago on the phenomenological grounds of molecular simulation [4,5], a rigorous proof or at least good heuristics to approach the problem mathematically are still lacking [6]. The topic has received a great deal of attention as a most basic example of entropy-driven phase transition [7,8] and the system itself is relevant to diverse areas of mathematics, physics, and other branches of the natural sciences and engineering [9,10]. Most remarkably, hard-sphere freezing is thought since pioneering work [11,12] to underlie the corresponding process for a simple substance whose particles interact via short-range forces. This has significantly contributed to conform the modern perspective of van der Waals original ideas highlighting the relevance of repulsive forces [13].

The van der Waals picture of freezing is different from its condensation counterpart insofar as in the former case the

transition is already displayed by the primitive hard-sphere system. Elucidating essential microscopic mechanisms underlying hard-sphere freezing is therefore highly advisable—Ising-like models appearing as a promising tool owing to their lattice-based nature and simplicity. In this connection, great effort has been devoted over decades to the class of hard-core lattice particle models [6,14–20]. These are two-state variants that start from the vacant-occupied site dichotomy characteristic of lattice gases and consider a $+\infty$ pair interaction potential that makes the presence of a particle in a given site to exclude occupancy of up to its k th neighbors—thereby mimicking the effects of harsh repulsive forces associated with hard molecular cores. A number of $k = 1$ versions in $d = 3$ are known to exhibit critical points [21] that are inconsistent with the strict first-order nature of freezing. While such undesired criticality is absent for certain variants with $k > 1$ [18], the possibility of getting an adequate description from an elementary $k = 1$ model is seemingly ruled out. This situation sharply contrasts with that for condensation, for which the standard lattice gas with $k = 1$ attraction [22] is known to perform reliably.

In the search for a most basic Ising prototype of the freezing transition, we introduce here a three-state model with $k = 1$ that pertains to the so-called Blume-Emery-Griffiths class [23,24]. On allowing particles to move in their respective “cells,” our approach crucially embraces *compressible cells* and *locally fluctuating free volumes* [25,26] to characterize a microscopic mechanism of molecular packing. This yields a phase transition akin to hard-sphere freezing together with an appropriate description of the thermodynamics of solid and fluid phases. An augmented variant consistently incorporating attractive interactions is then found to lead to every basic feature of the phase diagram of a simple substance. The statistical-mechanical treatment demands a great grand canonical ensemble associated with a completely open thermodynamic system [27]. We work at the mean-field level

^{*}jacobotc@uvigo.es[†]calvarez@uvigo.es

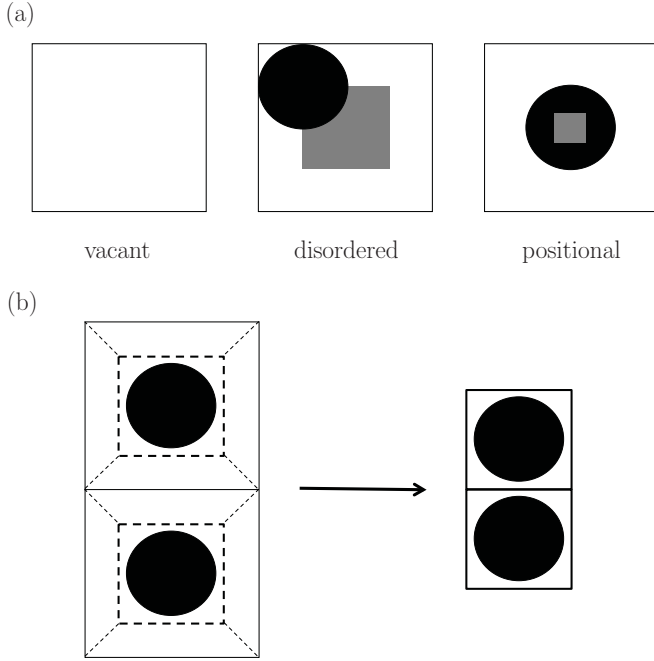


FIG. 1. Two-dimensional illustration of our hard-sphere model for a square lattice. (a) Individual cell states, with the shaded grey areas representing the free volume explored by particles in disordered and positional states (\dot{v}_0 and \dot{v}_1 , respectively). (b) Assembly of two nearest-neighbor cells containing particles with positional order; in the hypothetical case that all their six-nearest neighbors likewise contain particles with positional order, both cells receive inputs delimited by the isosceles trapezoids in the left graph to become the squares of reduced area in the right one.

throughout, with its inherent qualifications and limitations in mind.

The paper is organized as follows. The model is described in Sec. II, which also includes an account of the great grand canonical ensemble, the mean-field treatment, and the connection with thermodynamics. Numerical results are presented in Sec. III. Section IV summarizes our findings and discusses them in a broad context.

II. MODEL

A. Description

Consider the d -dimensional space divided into elementary cells of volume v_0 , each of which associated with a point of a Bravais lattice of coordination number c . As Fig. 1(a) illustrates, each cell can be in three states. In two of them, it can be empty or singly occupied in a disordered configuration by a hard sphere of diameter σ whose center explores a free volume $\dot{v}_0 < v_0$. In the remaining state, a particle just explores a preferential, restricted free volume $\dot{v}_1 < \dot{v}_0$ around the center of its cell. A molecular-packing mechanism is then implemented on simply postulating that the total volume of an assembly of two nearest-neighbor cells is decreased by $\delta v > 0$ when particles in them have the prescribed *positional order* [see Fig. 1(b)]. Packing is thus characterized by a $k = 1$ *entropy-volume coupling* involving cell's positional order. Such a coupling may be regarded ferromagneticlike inasmuch

as it contemplates a volume decrease. As a result, our packing mechanism is analogous to the one for condensation in the standard lattice gas, which entails a $k = 1$ *particle-energy coupling* involving cell's occupancy.

We shall impose the close-packed, static lattice picture to be recovered in the limiting case that all cells have positional order. This demands the lattice leading to close packing at the given d , but also the condition

$$v_0 - v_{cp} = \frac{c}{2} \delta v, \tag{1}$$

where v_{cp} stands for the volume per particle at close packing, while it is to be noted that $\frac{c}{2}$ is the number of nearest neighbors per cell. We may further consider

$$v_0 = \lambda_d \sigma^d, \quad v_{cp} = \gamma_d \sigma^d, \quad \text{and} \quad \dot{v}_1 = \omega_d \dot{v}_0, \tag{2}$$

with subscript d indicating that the corresponding parameter is d dependent. Note that $\lambda_d > 1$ and $\omega_d < 1$, while in, e.g., three dimensions one has the face-centered cubic lattice with $\gamma_3 = 1/\sqrt{2}$ corresponding to $\pi/3\sqrt{2} \approx 0.74$ for the customarily defined packing fraction.

The description of the hard-sphere piece of our model being completed, we further suppose that particles in nearest-neighbor cells attract each other. For every pair of adjacent occupied cells, there is a background interaction energy $-\varepsilon_0 < 0$ that is supplemented by an extra energy $-\delta\varepsilon < 0$ when both cells have positional order. In accord with standard conventions regarding dimensionality scalings [28], we shall consider

$$\varepsilon_0 = \frac{2}{c} a \quad \text{and} \quad \delta\varepsilon = \frac{2}{c} \delta a, \tag{3}$$

with c monotonically increasing with d .

The two ferromagneticlike couplings just introduced are consistent with a normal pair potential like the one due of Lennard-Jones and Devonshire. Specifically, the occupancy-related coupling has to do with the range at which the attractive piece of the pair potential becomes significant and is exactly the same underlying condensation in the standard lattice gas. On the other hand, the positional-related coupling mimics the minimum of the potential well.

B. Great grand canonical ensemble

The system's energy E , volume V , and number of particles N are all allowed to fluctuate simultaneously. A statistical-mechanical treatment thus embodies $e^{-\beta(E_i + pV_i - \mu N_i)}$ Boltzmann factors for microstates $\{I\}$, where p stands for the pressure and μ for the chemical potential while $\beta \equiv 1/k_B T$ with k_B the Boltzmann constant and T the temperature. Despite the corresponding great grand canonical ensemble being introduced long ago [27,29,30], only recently has its potential usefulness been illuminated [25,26,31–36]. Recalling its main features thus merits some attention.

The probability of a given microstate is [27,29,30,33]

$$p_I = \frac{e^{-\beta(E_i + pV_i - \mu N_i)}}{\Theta(T, p, \mu)}, \tag{4}$$

with

$$\Theta(T, p, \mu) = \sum_l e^{-\beta(E_l + pV_l - \mu N_l)}, \quad (5)$$

the corresponding partition function. As for averaged values, one finds from (4) and (5)

$$\langle N \rangle = \frac{1}{\beta} \left(\frac{\partial \ln \Theta}{\partial \mu} \right)_{T, p}, \quad \langle V \rangle = -\frac{1}{\beta} \left(\frac{\partial \ln \Theta}{\partial p} \right)_{T, \mu}, \quad (6)$$

and

$$\langle E \rangle = -\left(\frac{\partial \ln \Theta}{\partial \beta} \right)_{p, \mu} - p \langle V \rangle + \mu \langle N \rangle. \quad (7)$$

On the other hand, insertion of (4) into the standard formula relating $\{p_l\}$ to the entropy,

$$S = -k_B \sum_l p_l \ln p_l, \quad (8)$$

leads to

$$\langle E \rangle = TS - p \langle V \rangle + \mu \langle N \rangle - k_B T \ln \Theta. \quad (9)$$

We may express $\Theta(T, p, \mu)$ in terms of its associated grand canonical partition functions $\Xi(T, V, \mu)$ as

$$\Theta(T, p, \mu) = \sum_{V=V_{\min}}^{V_{\max}} e^{-\beta p V} \Xi(T, V, \mu), \quad (10)$$

where for \mathcal{N} cells

$$V_{\min} = \mathcal{N}v_{\text{cp}} \quad \text{and} \quad V_{\max} = \mathcal{N}v_0. \quad (11)$$

For a macroscopic system composed of particles interacting via short-range forces, all terms in the sum of (10) are nearly 1. This is so because $\Xi(T, V, \mu) = e^{\beta p(T, \mu)V}$, with the $p(T, \mu)$ function yielding the equilibrium pressure p corresponding to T and μ . In light of this, (10) leads to

$$\Theta(T, p, \mu) = \frac{c}{2} \mathcal{N} \quad (12)$$

because the gap between accessible volumes is δv and $(V_{\max} - V_{\min})/\delta v = \frac{c}{2} \mathcal{N}$ from (1) and (11).

Equation (12) is to be seen as indicating that $\Theta(T, p, \mu)$ is a function constrained to take an $O(\mathcal{N})$ constant value. Such an order of magnitude is a general property of the sum over microstates in the right-hand side of (5). Certainly, the sum is also $O(\mathcal{N})$ for microcanonical, canonical, and grand canonical ensembles, but only for the great grand canonical one does it identify with the associated partition function. We realize in Sec. IID that (12) crucially leads to a standard thermodynamic description.

C. Mean-field solution

We introduce spin-1 Ising variables $s_i = -1, 0, 1$, $i = 1, 2, \dots, \mathcal{N}$, characterizing the state of each cell, with $s_i = 0$ for a vacant cell, $s_i = -1$ for a cell containing a particle in a disordered configuration, and $s_i = 1$ for a cell containing a particle with positional order. We are then led to write

$$N\{s_i\} = \sum_{i=1}^{\mathcal{N}} s_i^2, \quad (13)$$

$$V\{s_i\} = \mathcal{N}v_0 - \delta v \sum_{\langle ij \rangle} \frac{s_i + 1}{2} \frac{s_j + 1}{2} s_i s_j, \quad (14)$$

and

$$E_p\{s_i\} = -\varepsilon_0 \sum_{\langle ij \rangle} s_i^2 s_j^2 - \delta \varepsilon \sum_{\langle ij \rangle} \frac{s_i + 1}{2} \frac{s_j + 1}{2} s_i s_j, \quad (15)$$

where E_p stands for the system's interaction potential energy.

On performing integrations over momenta and over the coordinates of each particle in its cell, we get for (5)

$$\begin{aligned} \Theta(T, p, \mu) = & \sum_{s_1=-1,0,1} \dots \sum_{s_{\mathcal{N}}=-1,0,1} \left(\frac{\dot{v}_0}{\Lambda^d} \right)^{\sum_{i=1}^{\mathcal{N}} \frac{s_i-1}{2} s_i} \\ & \times \left(\frac{\dot{v}_1}{\Lambda^d} \right)^{\sum_{i=1}^{\mathcal{N}} \frac{s_i+1}{2} s_i} e^{-\beta(E_p\{s_i\} + pV\{s_i\} - \mu N\{s_i\})}, \end{aligned} \quad (16)$$

where $\Lambda \equiv h/\sqrt{2\pi m k_B T}$ stands for the de Broglie thermal wavelength for a particle of mass m , with h the Planck's constant. It shall be useful to write

$$\Theta(T, p, \mu) = \sum_{s_1=-1,0,1} \dots \sum_{s_{\mathcal{N}}=-1,0,1} e^{-\beta \mathcal{H}\{s_i\}}, \quad (17)$$

where

$$\mathcal{H} = E_p + pV - \mu N - T S_{\text{fv}}, \quad (18)$$

with

$$S_{\text{fv}}\{s_i\} = k_B \left\{ \ln \left[\frac{(\dot{v}_0 \dot{v}_1)^{\frac{1}{2}}}{\Lambda^d} \right] \sum_{i=1}^{\mathcal{N}} s_i^2 + \frac{1}{2} \ln \omega_d \sum_{i=1}^{\mathcal{N}} s_i \right\}. \quad (19)$$

To evaluate \mathcal{H} , we first adopt

$$s_i = \langle s \rangle + \delta s_i \quad \text{and} \quad s_i^2 = \langle s^2 \rangle + \delta s_i^2, \quad (20)$$

with $\langle s \rangle$ and $\langle s^2 \rangle$ corresponding average values. On inserting these into (13)–(15) and (19), the standard mean-field calculation proceeds by neglecting $\delta s_i \delta s_j$, etc. terms. After some algebra, we get for (18)

$$\mathcal{H}\{s_i\} = \mathcal{N}K_0 - K_1 \sum_{i=1}^{\mathcal{N}} s_i^2 - K_2 \sum_{i=1}^{\mathcal{N}} s_i, \quad (21)$$

with

$$\begin{aligned} K_0 = & p\sigma^d \left[\lambda_d + \frac{1}{4}(\lambda_d - \gamma_d)(\langle s^2 \rangle + \langle s \rangle)^2 \right] \\ & + a \langle s^2 \rangle^2 + \frac{1}{4} \delta a (\langle s^2 \rangle + \langle s \rangle)^2, \end{aligned} \quad (22)$$

$$\begin{aligned} K_1 = & \frac{1}{2} p\sigma^d (\lambda_d - \gamma_d) (\langle s^2 \rangle + \langle s \rangle) + \mu \\ & + k_B T \ln \left[(\dot{v}_0 \dot{v}_1)^{\frac{1}{2}} \Lambda^{-d} \right] \\ & + 2 \left[a \langle s^2 \rangle + \frac{1}{4} \delta a (\langle s^2 \rangle + \langle s \rangle) \right], \end{aligned} \quad (23)$$

and

$$\begin{aligned} K_2 = & \frac{1}{2} p\sigma^d (\lambda_d - \gamma_d) (\langle s^2 \rangle + \langle s \rangle) \\ & + \frac{1}{2} k_B T \ln \omega_d + \frac{1}{2} \delta a (\langle s^2 \rangle + \langle s \rangle), \end{aligned} \quad (24)$$

as obtained with the aid of (1)–(3). This is only exact in the $d \rightarrow \infty$ limit and is generally assumed to be a reasonably good approximation for the $d = 3$ case of obvious physical interest.

Equations (17) and (21) carry a trivial factorization to get

$$\Theta = \{e^{-\beta K_0} [1 + e^{\beta(K_1+K_2)} + e^{\beta(K_1-K_2)}]\}^{\mathcal{N}}, \quad (25)$$

whose introduction into the exact relations

$$\langle s^2 \rangle = \frac{k_B T}{\mathcal{N}} \frac{\partial \ln \Theta}{\partial K_1} \quad \text{and} \quad \langle s \rangle = \frac{k_B T}{\mathcal{N}} \frac{\partial \ln \Theta}{\partial K_2} \quad (26)$$

leads to the self-consistency equations

$$\langle s^2 \rangle = \frac{e^{\beta(K_1+K_2)} + e^{\beta(K_1-K_2)}}{1 + e^{\beta(K_1+K_2)} + e^{\beta(K_1-K_2)}}, \quad (27)$$

$$\langle s \rangle = \frac{e^{\beta(K_1+K_2)} - e^{\beta(K_1-K_2)}}{1 + e^{\beta(K_1+K_2)} + e^{\beta(K_1-K_2)}}. \quad (28)$$

Being obtained from $\Theta(T, p, \mu)$, $\langle s^2 \rangle$ and $\langle s \rangle$ are functions of T , p , and μ and thereby imply that K_0 , K_1 , and K_2 in (22) to (24) are likewise functions of T , p , and μ .

D. Thermodynamic limit

We define

$$n \equiv \langle s^2 \rangle \quad \text{and} \quad n_- \equiv \frac{1}{2}(\langle s^2 \rangle + \langle s \rangle). \quad (29)$$

The former identifies to the overall fraction of occupied cells and is introduced for notational convenience, while the latter is the overall fraction of cells containing particles with positional order and notably simplifies (22) to (24). With these provisos, we conveniently rewrite (25) as

$$\frac{k_B T \ln \Theta}{\mathcal{N}} = -K_0 + k_B T \ln[1 + e^{\beta(K_1+K_2)} + e^{\beta(K_1-K_2)}]. \quad (30)$$

According to the definitions (6) and (7), this yields

$$\langle N \rangle = \mathcal{N}n, \quad (31)$$

$$\langle V \rangle = \mathcal{N}[\lambda_d - (\lambda_d - \gamma_d)n_-^2]\sigma^d, \quad (32)$$

and

$$\langle E \rangle = \mathcal{N} \left(\frac{d}{2} n k_B T - a n^2 - \delta a n_-^2 \right), \quad (33)$$

where we have used (22) to (24) [with (29)] while it is to be noted that all terms of the type $(\partial n / \partial T)_{p, \mu}$ cancel out.

At this stage, constraint (12) is taken into account. This implies that the left-hand side of (30) vanishes in the thermodynamic limit ($\mathcal{N} \rightarrow \infty$) since $\ln \Theta = O(\ln \mathcal{N})$. On accordingly equating the right-hand side to zero, we get

$$K_0 = k_B T \ln[1 + e^{\beta(K_1+K_2)} + e^{\beta(K_1-K_2)}], \quad (34)$$

which via the functional dependence of K_0 , K_1 , and K_2 on T , p , and μ provides the concrete form of the system's $Tp\mu$ relation.

Combination of (34) and (27) [with (22) to (24) and (29)] gives

$$p\sigma^d = - \frac{k_B T \ln(1-n) + a n^2 + \delta a n_-^2}{\lambda_d + (\lambda_d - \gamma_d)n_-^2}. \quad (35)$$

Similarly, (27) and (28) [with (22) to (24) and (29)] lead to

$$p\sigma^d = \frac{k_B T \ln\{n_- [\omega_d(n-n_-)]^{-1}\} - 2\delta a n_-}{2(\lambda - \gamma_d)n_-} \quad (36)$$

and

$$\mu = k_B T \{\ln(\nu_0^{-1} \Lambda^d) + \ln[(n-n_-)(1-n)^{-1}]\} - 2a n, \quad (37)$$

so from (35) and (36), one finds

$$T = \frac{a n^2 + \delta a n_-^2 - 2\delta a \Gamma n_-}{k_B \ln\{[\omega_d(n-n_-)n_-^{-1}]^\Gamma (1-n)^{-1}\}}, \quad (38)$$

with $\Gamma = [\lambda_d + (\lambda_d - \gamma_d)n_-^2] / [2(\lambda_d - \gamma_d)n_-]$.

Note from (31) to (33) that, in accord with extensivity, $\langle N \rangle$, $\langle V \rangle$, and $\langle E \rangle$ all scale with \mathcal{N} . Then, being $O(\ln \mathcal{N})$, $k_B T \ln \Theta$ may be regarded as *subextensive* and hence negligible in (9) when $\mathcal{N} \rightarrow \infty$, so the Euler equation holds in that limit. Furthermore, insertion of (31) to (33), (35), (37), and (38) into (9) gives for the entropy

$$S = \frac{d}{2} \mathcal{N} n k_B + S_{\text{fv}} + S_{\text{comb}}, \quad (39)$$

with

$$S_{\text{fv}} = \mathcal{N} k_B [n \ln(\nu_0 \Lambda^{-d}) + n_- \ln \omega_d], \quad (40)$$

and

$$S_{\text{comb}} = -\mathcal{N} k_B [n_- \ln n_- + (n-n_-) \ln(n-n_-) + (1-n) \ln(1-n)], \quad (41)$$

which render S likewise extensive. The free volume contribution (40) is of course equivalent to (19) and originates from the distinct positions available to particles in their respective cells. On the other hand, (41) is the standard combinatorial formula associated with the distinct number of ways of distributing the three types of cells along the lattice.

We may finally note that the differential relation $d \ln \Theta = (\partial \ln \Theta / \partial T)_{p, \mu} dT + (\partial \ln \Theta / \partial p)_{T, \mu} dp + (\partial \ln \Theta / \partial \mu)_{T, p} d\mu$ leads, in light of (6), (7), (9), and (12), to Gibbs-Duhem relation

$$0 = SdT - \langle V \rangle dp + \langle N \rangle d\mu. \quad (42)$$

We therefore meet all aspects of the standard thermodynamic description expected for the systems with short-range interactions of our current interest.

III. NUMERICAL RESULTS

A. Hard-sphere system

The hard-sphere system is characterized by $a = \delta a = 0$. This implies that both p and T cancel out when (35) and (36) are combined, so we actually have in place of (38):

$$\frac{\lambda_d + (\lambda_d - \gamma_d)n_-^2}{2(\lambda_d - \gamma_d)n_-} = \frac{\ln(1-n)}{\ln[\omega_d(n-n_-)n_-^{-1}]}. \quad (43)$$

On the other hand, the expression for the number density $\rho \equiv \langle N \rangle / \langle V \rangle$ is from (31) and (32):

$$\rho \sigma^d = \frac{n}{\lambda_d - (\lambda_d - \gamma_d)n_-^2}. \quad (44)$$

The joint consideration of (43) and (44) indicates that only one among $\rho \sigma^3$, n , and n_- is independent. This implies that

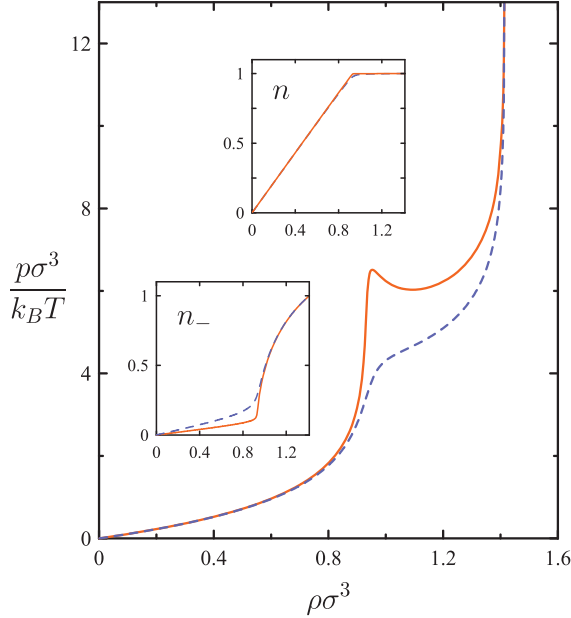


FIG. 2. Hard-sphere $d = 3$ model behavior as obtained from calculations explained in Sec. III A. The order parameters n and n_- in the insets are plotted as a function of $\rho\sigma^3$ too. Orange solid curves correspond to $\omega_3 = 0.1$ and blue dashed ones to $\omega_3 = 0.2$, with $\lambda_3 = 1.08$ in both cases.

(35) and (36) (with $a = \delta a = 0$) are, in practice, of the form $p/k_B T = f(\rho)$, as statistical mechanics demands for a hard-sphere system [37].

To obtain numerical results, one may first prescribe d and, concomitantly, γ_d . We shall focus on the $d = 3$ case, for which the face-centered cubic lattice with $\gamma_3 = 1/\sqrt{2}$ is to be selected (cf. Sec. II A). Then, for each given $\rho\sigma^3$ value, one may solve (43) and (44) for n and n_- to finally obtain the corresponding $p\sigma^3/k_B T$ value from (35). Figure 2 shows that the corresponding $p\sigma^3/k_B T$ vs $\rho\sigma^3$ curve exhibits a van der Waals loop when ω_3 is small enough. This is known to be the signature of a phase transition, which we identify with freezing. It is important to note that $\rho\sigma^3$ always changes discontinuously from one coexisting phase to another, implying that the transition is strictly first-order (i.e., no critical point). The standard graphical analysis of Fig. 3 further illustrates this point.

Note also from Fig. 2 that $n \approx 1$ along coexistence. This implies that the transition originates from a two-state model with disordered and positional cells, in which n_- acts as an order parameter of entropic nature [cf. (40)]. In this connection, the up-down symmetry of the underlying Ising model implies that the coexisting phases fulfill $(n_-)_{\text{fluid}} + (n_-)_{\text{crystal}} \approx 1$. It then turns out from (31) and (39) to (41) that

$$\frac{S_{\text{fluid}} - S_{\text{crystal}}}{Nk_B} \approx -\frac{1}{2} \ln \omega_d. \quad (45)$$

Accordingly, $\omega_3 = 0.1$ was chosen so as to meet the $(S_{\text{fluid}} - S_{\text{crystal}})/Nk_B \approx 1.16$ value determined from molecular simulation [38]. On the other hand, we got an optimal $\lambda_3 = 1.08$ value yielding the simulated $(\rho\sigma^3)_{\text{fluid}} \approx 0.938$ result [39].

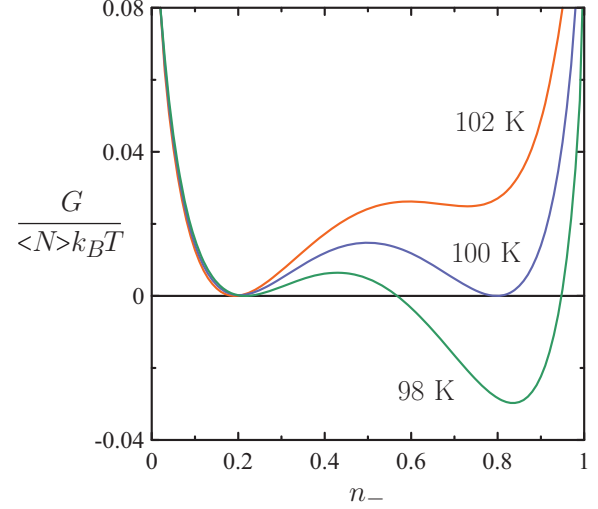


FIG. 3. Scaled Gibbs free energy per particle, with $G = \langle E \rangle - TS + p\langle V \rangle$, for hard spheres of diameter $\sigma = 3 \text{ \AA}$ and mass $m = 3 \times 10^{-26} \text{ kg}$ in $d = 3$ as obtained from (31) to (33) and (39) to (41) as a function of the order parameter n_- at $p = 3160 \text{ bar}$ and temperatures indicated explicitly. The stable phase is at 98 K the one with higher n_- (solid) and at 102 K the one with lower n_- (fluid). Solid-fluid coexistence occurs at 100 K at the selected p . This picture, characterized by a finite difference between the n_- values of the coexisting phases, remains for any path crossing the coexistence curve in the p - T plane. Note that curves have been conveniently shifted so as to get a common $G/\langle N \rangle k_B T$ value at the minimum corresponding to lower n_- .

These values of ω_3 and λ_3 lead to $(\rho\sigma^3)_{\text{crystal}} \approx 1.186$, which departs from the 1.037 simulated one [39].

While one may hope to get a closer numerical estimate of $(\rho\sigma^3)_{\text{crystal}}$ by further refining the model beyond its oversimplified description of the excluded-volume problem, such an expediency is outside the scope of the present paper. In any event, the quantitative discrepancy between the values in Fig. 2 and simulation data is nothing surprising inasmuch as a mean-field treatment is only exact in the $d \rightarrow \infty$ limit. A further caveat regarding our mean-field approach concerns nonadditivity, which has been shown to make Blume-Emery-Griffiths models to exhibit ensemble inequivalence and negative heat capacities for certain ranges of parameter values [40]. These peculiarities, unrealistic for the systems with short-range interactions of our current interest, are fortunately absent for the parameter setting adopted here to accommodate freezing.

B. Simple substance

We now consider the $d = 3$ model with added attractive interactions ($a, \delta a \neq 0$) and focus on its capability to describe the phase behavior of a simple substance like argon, for which the Lennard-Jones potential is known to perform reliably. Thus, with the same values of λ_3 and ω_3 quoted in Sec. III A, we choose values for σ , a , and δa consistent with argon's Lennard-Jones parameters. In particular, on starting from $\sigma_{\text{LJ}}^{\text{argon}} \approx 3.4 \text{ \AA}$ and $\varepsilon_{\text{LJ}}^{\text{argon}} \approx 0.0103 \text{ eV}$ [42], we set $\sigma = \sigma_{\text{LJ}}^{\text{argon}}$

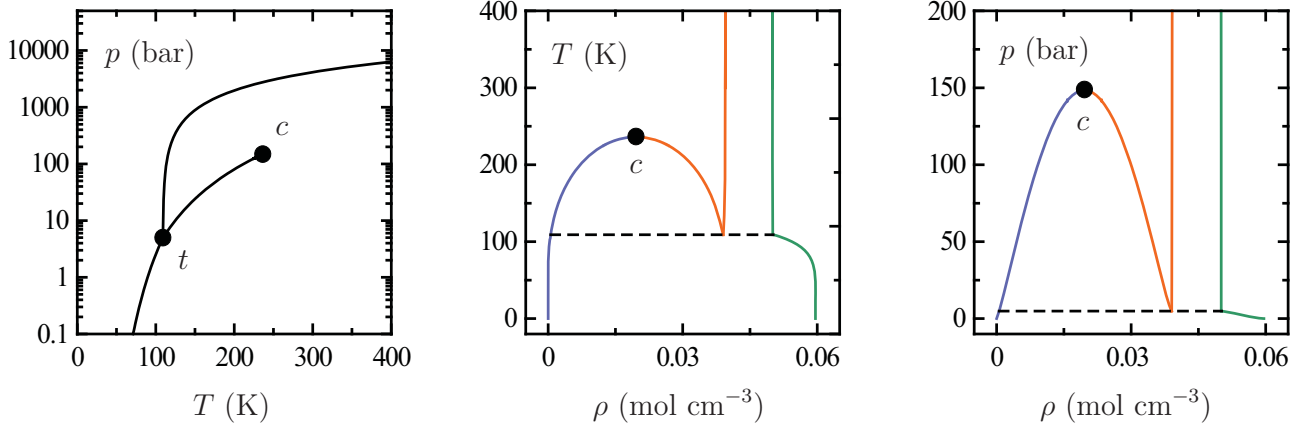


FIG. 4. Phase diagram for the simple-substance model in the p - T , T - ρ , and p - ρ planes as obtained from calculations explained in Sec. III B. Lines in the p - T plane determine the conditions of two-phase coexistence bounded by the triple point t and the gas-liquid critical point c . Lines in the T - ρ and p - ρ planes enclose regions of two-phase coexistence for crystal (green), liquid (orange), and gas (blue), with horizontal dashed lines joining the states of three-phase coexistence associated with t . The model's values for the triple-point temperature and melting enthalpy are, respectively, $T_t \approx 110$ K and $\Delta h_{\text{melting}} \approx 1.4$ kJ mol $^{-1}$, their experimental counterparts being $T_t \approx 84$ K and $\Delta h_{\text{melting}} \approx 1.2$ kJ mol $^{-1}$ [41].

and choose optimal $a \simeq 0.04044$ eV and $\delta a \simeq 0.02178$ eV values fulfilling $\varepsilon_0 + \delta\varepsilon = \varepsilon_{\text{LJ}}^{\text{argon}}$ [cf. (3) with $c = 12$].

To obtain the phase behavior, we may impose the conditions of isothermal coexistence $\mu(T, \rho') = \mu(T, \rho'')$ and $p(T, \rho') = p(T, \rho'')$. Note, however, that explicit $p(T, \rho)$ and $\mu(T, \rho)$ expressions are precluded by the dependence of the model's equations on n and n_- (see Sec. II D). Thus, given T and ρ , one may first solve (38) and (44) for n and n_- to then get $p(T, \rho)$ and $\mu(T, \rho)$ from (35) and (37). With this prescription, conditions of two-phase coexistence are met with the aid of standard recipes.

Figure 4 shows that the resulting phase diagrams display all basic features revealed by experiment. The figure's caption specifies that the model compares favorably (at a semiquantitative level) with argon's experimental data. A qualitative difference is the symmetry of the gas-liquid and solid-liquid coexistence curves in the T - ρ and p - ρ planes, reminiscent of the up-down symmetry of the underlying Ising model but absent in experimental data. Note also in passing that further calculations (not shown here) indicate that our classical model qualitatively describes the thermodynamics of the solid phase at sufficiently high temperatures for quantum effects to be of no major relevance.

We have checked that around gas-liquid criticality, our three-state model reduces to a standard lattice gas with interaction energy $-\varepsilon_0$. The fairly reliable picture of Fig. 4 is thus not surprising as condensation is concerned. It is, however, a remarkable result for freezing. Crucial to this transition is its primitive hard-sphere counterpart discussed in Sec. III A. An additional relevant feature is the coupling of $-\delta\varepsilon$ with positional order, which, as described in Sec. II A, consistently characterizes the minimum of the Lennard-Jones potential underlying simple substances.

IV. SUMMARY AND DISCUSSION

A d -dimensional three-state Ising model has been described in Sec. II A. In addition to the standard distinction

between occupied and empty cells, it considers cells containing particles exploring a restricted free volume. Such positional-order cells serve to feature molecular packing via an *entropy-volume* coupling of ferromagneticlike nature just involving first neighbors. This characterization of the effects of harsh repulsive forces is in sharp contrast with the one provided by hard-core lattice particle models, which approach the problem via an antiferromagnetic coupling of energetic nature that needs to be extended beyond first neighbors [6,14–20]. Our most basic model is aimed to describe the hard-sphere system and, as specified in Sec. II A, leads to an augmented version for a simple substance when attractive interactions are incorporated in a way consistent with a normal pair potential like the one due to Lennard-Jones and Devonshire. Since the nature of our assumptions entails the system's energy, volume, and number of particles to fluctuate simultaneously, a statistical-mechanical treatment demands working in the great grand canonical ensemble described in Sec. II B. This has been accomplished at a mean-field level as explained in Sec. II C, while the connection with thermodynamics is made in Sec. II D.

As shown in Sec. III A, the primitive model with no attractive interactions exhibits a single phase transition akin to the freezing of the hard-sphere fluid in $d = 3$ earlier revealed by molecular simulation [4,5]. The model accounts for the strict first-order nature of freezing [43,44]. In this connection, we stress that a strictly first-order transition has been accommodated in a framework—the Ising framework—traditionally paradigmatic for the critical point. We speculate that this nontrivial result originates from the entropic nature of the transition's positional order parameter.

The model's version perturbatively incorporating attractive interactions has been found in Sec. III B to exhibit a behavior qualitatively consistent with all experimentally known basic attributes of the phase diagram of a simple substance. This perseveres on the contemporary perspective of van der Waals theory, indicating that switching on attractive interactions in a reference hard-sphere system suffices to describe the

thermodynamics of a simple substance. Such a picture was envisioned for freezing by Longuet-Higgins and Widom [11,12], who, however, started from the corrected equation of state of hard-spheres provided by molecular simulation [4]. Our present approach develops such a van der Waals picture by preliminarily meeting the hard-sphere phenomenology from first principles of statistical mechanics.

The nice accord with evidence arising from experiment and simulation makes it tempting to speculate that our model may constitute an adequate Ising prototype of freezing. Furthermore, such a piece of phenomenological consistency plausibly renders the in-effect $d \rightarrow \infty$ mean-field solutions so far explored a reasonable approximation for freezing in $d = 3$. Mean-field theory thus appears again as a sensible approximation of the three-dimensional world, just as found for condensation since van der Waals's early work and conjectured for glass and jamming phenomenology in the latest theory of simple glasses [28]. One obvious benefit of our mean-field approach is that it suggests freezing to persist in infinitely many dimensions, as claimed recently from simulations proving that the hard-sphere phase diagram retains its $d = 3$ main features up to $d = 10$ [45].

An open question regarding our mean-field treatment is whether it may eventually lead to undesired features associated with nonadditivity such as ensemble inequivalence or negative heat capacities. There is an expectation [46] that avoidance of such features demands the thermodynamic limit to be taken before the mean-field one. Since our present approach considers the mean-field limit first, it turns out that ensemble inequivalence, etc. are to be expected. Therefore, while we have not observed any trace of these features for the parameter setting adopted, there might be ranges of parameter values for which they arise as it indeed happens for systems with long-range interactions [40].

It is to be emphasized that the great grand canonical ensemble employed, while seldom used for decades, is increasingly receiving attention to provide satisfactory solutions to long-standing problems such as the Yang-Yang anomaly in fluid criticality [25,26], the unusual thermodynamics of liquid and supercooled water [31,34], or the elementary freezing transition targeted in this paper. A fully unconstrained ensemble in which temperature, pressure, and chemical potential are *independently* fixed has recently proved useful for problems involving long-range interactions such as they occur, e.g., in self-gravitating systems [33,35,36]. There is thus a suggestion that consideration of systems in completely open environments may constitute a step further in our statistical-mechanical characterization of the physical world.

Future work entails analyzing the validity range of the model's mean-field solutions. An obvious expediency in this connection would be to get the model's exact solutions for finite d with the aid of molecular simulation. Likewise, it would be appealing to accomplish a study of the nonadditivity problem paralleling work developed over the years for systems with long-range interactions [47,48]. It would also be natural to further extend the investigation to substances beyond the van der Waals paradigm. One prominent candidate is water, for which incorporation of the orientational degrees of freedom associated with hydrogen bonding looks promising [34]. Work on some of these issues is currently in progress.

ACKNOWLEDGMENTS

We are grateful to F. Zamponi for useful comments on the conditions at which nonadditivity-related issues may show up in infinite dimensions. Support from the Spanish Ministry of Science, Innovation, and Universities under Grant No. PID2020-115722GB-C22 is greatly acknowledged.

-
- [1] N. W. Ashcroft and N. D. Mermin, *Solid State Physics* (Saunders College Publishing, New York, 1976).
 - [2] J. M. Kosterlitz and D. J. Thouless, Early work on defect-mediated phase transitions, *Int. J. Mod. Phys. B* **30**, 1630018 (2016).
 - [3] M. Baus, The present status of the density functional theory of the liquid-solid transition, *J. Phys.: Condens. Matter* **2**, 2111 (1990).
 - [4] B. Alder and T. Wainwright, Phase transition for a hard sphere system, *J. Chem. Phys.* **27**, 1208 (1957).
 - [5] W. W. Wood and J. D. Jacobson, Preliminary results from a recalculation of the Monte Carlo equation of state of hard spheres, *J. Chem. Phys.* **27**, 1207 (1957).
 - [6] I. Jauslin and J. L. Lebowitz, High-fugacity expansion, Lee-Yang zeros and order-disorder transitions in hard-core lattice systems, *Commun. Math. Phys.* **364**, 655 (2018).
 - [7] D. Frenkel, Order through entropy, *Nat. Mater.* **14**, 9 (2015).
 - [8] F. Sciortino, Entropy in self-assembly, *Riv. Nuovo Cimento* **42**, 511 (2019).
 - [9] G. Parisi and F. Zamponi, Mean-field theory of hard sphere glasses and jamming, *Rev. Mod. Phys.* **82**, 789 (2010).
 - [10] S. Torquato and F. H. Stillinger, Jammed hard-particle packings: From Kepler to Bernal and beyond, *Rev. Mod. Phys.* **82**, 2633 (2010).
 - [11] H. C. Longuet-Higgins and B. Widom, A rigid sphere model for melting of argon, *Mol. Phys.* **8**, 549 (1964).
 - [12] B. Widom, Intermolecular forces and the nature of the liquid state, *Science* **157**, 375 (1967).
 - [13] D. Chandler, J. D. Weeks, and H. C. Andersen, Van der Waals picture of liquids, solids, and phase transformations, *Science* **220**, 787 (1983).
 - [14] C. Domb, Some theoretical aspects of melting, *Nuovo Cimento* **9**, 9 (1958).
 - [15] D. S. Gaunt and M. E. Fisher, Hard-sphere lattice gases. I. Plane-square lattice, *J. Chem. Phys.* **43**, 2840 (1965).
 - [16] A. Bellemans and R. K. Nigam, Phase transitions in two-dimensional lattice gases of hard-square molecules, *J. Chem. Phys.* **46**, 2922 (1967).
 - [17] R. J. Baxter, Hard hexagons: Exact solution, *J. Phys. A: Math. Gen.* **13**, L61 (1980).
 - [18] A. Z. Panagiotopoulos, Thermodynamic properties of lattice hard-sphere models, *J. Chem. Phys.* **123**, 104504 (2005).

- [19] N. Vigneshwar, D. Mandal, K. Damle, D. Dhar, and R. Rajesh, Phase diagram of a system of hard cubes on the cubic lattice, *Phys. Rev. E* **99**, 052129 (2019).
- [20] A. A. A. Jaleel, D. Mandal, J. E. Thomas, and R. Rajesh, Freezing phase transition in hard-core lattice gases on the triangular lattice with exclusion up to seventh next-nearest neighbor, *Phys. Rev. E* **106**, 044136 (2022).
- [21] D. S. Gaunt, Hard-Sphere Lattice gases. II. Plane-triangular and three-dimensional lattices, *J. Chem. Phys.* **46**, 3237 (1967).
- [22] T. D. Lee and C. N. Yang, Statistical theory of equations of state and phase transitions. II. Lattice gas and Ising model, *Phys. Rev.* **87**, 410 (1952).
- [23] M. Blume, V. J. Emery, and R. B. Griffiths, Ising model for the lambda transition and phase separation in $\text{He}^3\text{-He}^4$ mixtures, *Phys. Rev. A* **4**, 1071 (1971).
- [24] D. Mukamel and M. Blume, Ising model for tricritical points in ternary mixtures, *Phys. Rev. A* **10**, 610 (1974).
- [25] C. A. Cerdeiriña, G. Orkoulas, and M. E. Fisher, Soluble model fluids with complete scaling and Yang-Yang features, *Phys. Rev. Lett.* **116**, 040601 (2016).
- [26] C. A. Cerdeiriña and G. Orkoulas, Compressible cell gas models for asymmetric fluid criticality, *Phys. Rev. E* **95**, 032105 (2017).
- [27] E. A. Guggenheim, *Thermodynamics*, 2nd ed. (North Holland, Amsterdam, 1950).
- [28] G. Parisi, P. Urbani, and F. Zamponi, *Theory of Simple Glasses. Exact Solutions in Infinite Dimensions* (Cambridge University Press, Cambridge, 2020).
- [29] T. L. Hill, *Statistical Mechanics. Principles and Selected Applications* (McGraw-Hill, New York, 1956), Sec. 14, Appendixes 2 and 4.
- [30] R. A. Sack, Pressure-dependent partition functions, *Mol. Phys.* **2**, 8 (1959).
- [31] S. Sastry, P. G. Debenedetti, F. Sciortino, and H. E. Stanley, Singularity-free interpretation of the thermodynamics of supercooled water, *Phys. Rev. E* **53**, 6144 (1996).
- [32] G. Orkoulas and D. P. Noon, Spatial updating in the great grand canonical ensemble, *J. Chem. Phys.* **131**, 161106 (2009).
- [33] I. Latella, A. Pérez-Madrid, A. Campa, L. Casetti, and S. Ruffo, Long-range interacting systems in the unconstrained ensemble, *Phys. Rev. E* **95**, 012140 (2017).
- [34] C. A. Cerdeiriña, J. Troncoso, D. González-Salgado, P. G. Debenedetti, and H. E. Stanley, Water's two-critical-point scenario in the Ising paradigm, *J. Chem. Phys.* **150**, 244509 (2019).
- [35] A. Campa, L. Casetti, I. Latella, and S. Ruffo, Phase transitions in the unconstrained ensemble, *J. Stat. Mech.: Theory Exp.* **2020**, 014004 (2020).
- [36] I. Latella, A. Campa, L. Casetti, P. Di Cintio, J. M. Rubí, and S. Ruffo, Monte Carlo simulations in the unconstrained ensemble, *Phys. Rev. E* **103**, L061303 (2021).
- [37] P. A. Monson and D. A. Kofke, Solid-fluid equilibrium: Insights from simple molecular models, in *Advances in Chemical Physics*, edited by I. Prigogine and S. A. Rice, Vol. 115 (John Wiley and Sons, New York, 2000), pp. 113–179.
- [38] F. H. Stillinger, P. G. Debenedetti, and T. M. Truskett, The Kauzmann paradox revisited, *J. Phys. Chem. B* **105**, 11809 (2001).
- [39] M. Robles, M. López de Haro, and A. Santos, Equation of state and the freezing point in the hard-sphere model, *J. Chem. Phys.* **140**, 136101 (2014).
- [40] A. Campa, T. Dauxois, and S. Ruffo, Statistical mechanics and dynamics of solvable models with long-range interactions, *Phys. Rep.* **480**, 57 (2009).
- [41] E. W. Lemmon, I. H. Bell, M. L. Huber, and M. O. McLinden, Thermophysical properties of fluid systems, in *NIST Standard Reference Database Number 69*, edited by P.J. Linstrom and W. G. Mallard (National Institute of Standards and Technology, Gaithersburg, MD, 2023).
- [42] J.-P. Hansen and I. R. McDonald, *Theory of Simple Liquids*, 3rd Ed. (Academic Press, Amsterdam, 2006).
- [43] *Collected Papers of L. D. Landau*, edited by D. Ter Haar (Gordon and Breach, New York, 1965), Chap. 29.
- [44] K. Binder, Theory of first-order phase transitions, *Rep. Prog. Phys.* **50**, 783 (1987).
- [45] P. Charbonneau, C. M. Gish, R. S. Hoy, and P. K. Morse, Thermodynamic stability of hard sphere crystals in dimensions 3 through 10, *Eur. Phys. J. E* **44**, 101 (2021).
- [46] F. Zamponi (Private Communication).
- [47] J. Barré, D. Mukamel, and S. Ruffo, Inequivalence of ensembles in a system with long-range interactions, *Phys. Rev. Lett.* **87**, 030601 (2001).
- [48] V. V. Prasad, A. Campa, D. Mukamel, and S. Ruffo, Ensemble inequivalence in the Blume-Emery-Griffiths model near a fourth-order critical point, *Phys. Rev. E* **100**, 052135 (2019).